

Operator Splitting for Three-Phase Flow in Heterogeneous Porous Media

E. Abreu¹, J. Douglas^{2,*}, F. Furtado³ and F. Pereira⁴

¹ Instituto Nacional de Matemática Pura e Aplicada, RJ 22460-320, Brazil.

² Department of Mathematics, Purdue University, West Lafayette, IN 47907-1395, USA.

³ Department of Mathematics, University of Wyoming, Laramie, WY 82071-3036, USA.

⁴ Department of Mathematics and School of Energy Resources, University of Wyoming, Laramie, WY 82071-3036, USA.

Received 7 November 2007; Accepted (in revised version) 17 July 2008

Available online 18 November 2008

Abstract. We describe an operator splitting technique based on physics rather than on dimension for the numerical solution of a nonlinear system of partial differential equations which models three-phase flow through heterogeneous porous media. The model for three-phase flow considered in this work takes into account capillary forces, general relations for the relative permeability functions and variable porosity and permeability fields. In our numerical procedure a high resolution, nonoscillatory, second order, conservative central difference scheme is used for the approximation of the nonlinear system of hyperbolic conservation laws modeling the convective transport of the fluid phases. This scheme is combined with locally conservative mixed finite elements for the numerical solution of the parabolic and elliptic problems associated with the diffusive transport of fluid phases and the pressure-velocity problem. This numerical procedure has been used to investigate the existence and stability of nonclassical shock waves (called transitional or undercompressive shock waves) in two-dimensional heterogeneous flows, thereby extending previous results for one-dimensional flow problems. Numerical experiments indicate that the operator splitting technique discussed here leads to computational efficiency and accurate numerical results.

AMS subject classifications: 76S05, 76T30, 78M10, 78M20

Key words: Operator splitting, three-phase flow, heterogeneous porous media, central differencing schemes, mixed finite elements.

1 Introduction

The study of operator splitting techniques has a long history and has been pursued with various methods. Since alternating-direction methods were introduced by Douglas,

*Corresponding author. Email addresses: eabreu@impa.br (E. Abreu), douglas@math.purdue.edu (J. Douglas), furtado@uwy.edu (F. Furtado), lpereira@uwy.edu (F. Pereira)

Peaceman and Rachford [1–5] and fractional step methods by D'jakonov, Marchuk and Yanenko [6, 7], these procedures, which reduce the time-stepping of multidimensional problems to locally one-dimensional computations, have been applied in the numerical simulation of many physically important problems, including reservoir flow problems, particularly in the case of single and two-phase flows. Here, the operator splitting is based on separating the underlying physical processes and treating each such process appropriately; thus, instead of solving the governing differential equations in the form which results directly from the basic conservation laws (supplemented by constitutive relations), the system of equations will be rewritten in such a way as to exhibit clearly each physical process. Then, distinct, appropriate numerical techniques can be orchestrated within an operator-splitting formulation to furnish effective and efficient numerical procedures designed to resolve the sharp gradients and dynamics evolving at vastly different rates which are the hallmarks of reservoir flow problems.

We present an operator splitting technique for the numerical solution of a highly nonlinear system of differential equations modeling three-phase flow through heterogeneous porous media. Three-phase flow in porous media is important in a number of scientific and technological contexts, including enhanced oil recovery [8–14], geological CO₂ sequestration [15], and radionuclide migration from repositories of nuclear waste [16, 17].

We consider the governing system of equations written in terms of the oil pressure (see, e.g., [18, 19]); this formulation allows us to identify a subsystem of nonlinear hyperbolic conservation laws (associated with convective transport), a parabolic subsystem of equations (associated with diffusive transport), and a elliptic subsystem (associated with the pressure-velocity calculation). Our splitting procedure solves the elliptic, hyperbolic, and parabolic subsystems sequentially, using numerical methods specifically tailored to such types of partial differential equations. We remark that it would have been very difficult, if not impossible, to employ such state-of-the-art numerical schemes had we attempted to solve the original system by standard implicit procedures. Moreover, any implicit procedure would require considerably more expensive computations since large linear and nonlinear problems, which do not appear in the splitting scheme, would have to be treated. Our splitting technique allows time steps for the pressure-velocity calculation that are longer than those for the diffusive calculation, which, in turn, can be longer than those for convection.

For three-phase flow, distinct empirical models have been proposed for the relative permeability functions [20–22], and more recently [23]. In addition, it is well known that for some of these models [20–22], which have been used extensively in petroleum engineering, the 2×2 system of conservation laws (the saturation equations) that arises when capillarity (diffusive) effects are neglected fails to be strictly hyperbolic somewhere in the interior of the saturation triangle (the phase space). This loss of strict hyperbolicity frequently leads to the occurrence of nonclassical shock waves (called transitional or undercompressive shock waves) in the solutions of the three-phase flow model. Crucial to calculating transitional shock waves is the correct modeling of capillarity effects [24]. Thus, their accurate computation constitutes a *bona fide* test for numerical simulators.

Different approaches for solving numerically the three-phase flow equations are discussed in [19, 25–27].

The rest of this paper is organized as follows. In Section 2 we introduce the model for three-phase flow in heterogeneous porous media that we consider. In Section 3 we discuss our operator splitting strategy for solving the three-phase flow system. In Section 4 we present computational solutions for the model problem considered here. Conclusions appear in Section 5.

2 Three-phase flow system

We consider two-dimensional flow of three immiscible, incompressible fluid phases in a porous medium. The phases will be referred to as water, gas, and oil and indicated by the subscripts w , g , and o , respectively. We assume that there are no internal sources or sinks. Compressibility, mass transfer between phases, and thermal effects are neglected. We assume that the three fluid phases saturate the pores; thus, with S_i denoting the saturation (local volume fraction of the pore space) of phase i ,

$$\sum_{i=w,g,o} S_i = 1. \quad (2.1)$$

Consequently, any pair of saturations inside the triangle

$$\Delta := \{(S_i, S_j) : S_i, S_j \geq 0, S_i + S_j \leq 1, i \neq j\}$$

of saturations can be chosen to describe the state of the fluid.

We refer the reader to [18, 19, 29] for a detailed description of the derivation of the phase formulation of the governing equations of three-phase flow. In our model we shall work with the saturations S_w and S_g of water and gas, respectively. Then, the equations describing conservation of mass of water and gas are

$$\frac{\partial}{\partial t} [\phi(\mathbf{x}) S_w] + \nabla \cdot [\mathbf{v} f_w(S_w, S_g)] = \nabla \cdot \mathbf{w}_w, \quad (2.2)$$

$$\frac{\partial}{\partial t} [\phi(\mathbf{x}) S_g] + \nabla \cdot [\mathbf{v} f_g(S_w, S_g)] = \nabla \cdot \mathbf{w}_g. \quad (2.3)$$

The diffusion terms \mathbf{w}_w and \mathbf{w}_g that arise in the saturation equations above, because of capillary pressure differences, are given by

$$[\mathbf{w}_w, \mathbf{w}_g]^T = K(\mathbf{x}) B(S_w, S_g) [\nabla S_w, \nabla S_g]^T. \quad (2.4)$$

In (2.4), $[\mathbf{a}, \mathbf{b}]$ denotes the 2-by-2 matrix with column vectors \mathbf{a} and \mathbf{b} , and $B(S_w, S_g) = Q P'$, where

$$Q(S_w, S_g) = \begin{bmatrix} \lambda_w(1-f_w) & -\lambda_w f_g \\ -\lambda_g f_w & \lambda_g(1-f_g) \end{bmatrix}, \quad P'(S_w, S_g) = \begin{bmatrix} \frac{\partial p_{wo}}{\partial S_w} & \frac{\partial p_{wo}}{\partial S_g} \\ \frac{\partial p_{go}}{\partial S_w} & \frac{\partial p_{go}}{\partial S_g} \end{bmatrix}. \quad (2.5)$$

Here, $K(\mathbf{x})$ and $\phi(\mathbf{x})$ are the absolute permeability and the porosity of the porous medium, respectively;

$$\lambda_i(S_w, S_g) = k_i / \mu_i, \quad i = w, g,$$

denote the phase mobilities, given in terms of the phase relative permeabilities k_i and phase viscosities μ_i . The fractional flow function of phase i is given by

$$f_i(S_w, S_g) = \lambda_i / \lambda, \quad \lambda = \lambda_g + \lambda_o + \lambda_w.$$

The capillary pressures

$$p_{ij} = p_i - p_j, \quad i \neq j,$$

where p_i is the pressure in phase i , are assumed to depend solely on the saturations.

The pressure-velocity equations associated with the three-phase flow system are

$$\nabla \cdot \mathbf{v} = 0, \quad (2.6)$$

$$\mathbf{v} = -K(\mathbf{x})\lambda(S_w, S_g)\nabla p_o + \mathbf{v}_{wo} + \mathbf{v}_{go}, \quad (2.7)$$

where \mathbf{v}_{wo} and \mathbf{v}_{go} , the “velocity corrections” due to capillary pressure differences, are defined by

$$\mathbf{v}_{io} = -K(\mathbf{x})\lambda_i(S_w, S_g)\nabla p_{io}, \quad i = w, g. \quad (2.8)$$

Boundary and initial conditions for the three-phase flow system of Eqs. (2.2)-(2.8), to be imposed below, complete the definition of the mathematical model. In particular, S_w and S_g must be specified at the initial time $t=0$.

3 Operator splitting for the three-phase flow system

We employ a two-level operator-splitting procedure for the numerical solution of the three-phase flow system (2.2)-(2.8) in which we first split the pressure-velocity calculation from the saturation calculation and then split the saturation calculation into convection and diffusion. The splitting allows time steps for the pressure-velocity calculation that are longer than those for the diffusive calculation, which are in turn longer than those for convection. Thus, we introduce three time steps: Δt_c for the solution of the hyperbolic problem for the convection, Δt_d for the parabolic problem for the diffusive calculation and Δt_p for the elliptic problem for the pressure-velocity calculation:

$$\Delta t_p = i_1 \Delta t_d = i_1 i_2 \Delta t_c, \quad (3.1)$$

where i_1 and i_2 are positive integers, so that $\Delta t_p \geq \Delta t_d \geq \Delta t_c$. Let

$$t^m = m \Delta t_p, \quad t_n = n \Delta t_d \quad \text{and} \quad t_{n,\kappa} = t_n + \kappa \Delta t_c, \quad 0 \leq \kappa \leq i_2, \quad (3.2)$$

so that $t_{n,i_2} = t_{n+1}$. Then, given a generic function z , denote its values at times t^m , t_n , and $t_{n,\kappa}$ by z^m , z_n , and $z_{n,\kappa}$, respectively.

In practice, variable time steps are always useful, especially for the convection microsteps subject dynamically to a Courant-Friedrichs-Lowy (CFL) restriction. To simplify the description of the operator splitting, assume each time step to have a single value.

The oil pressure (and Darcy velocity) will be approximated at times t^m , $m=0,1,2,\dots$. The saturations, S_w and S_g , will be approximated at times t_n , $n=1,2,\dots$; recall that they need to be specified at $t=0$. In addition, there will be values for the saturation computed at intermediate times $t_{n,\kappa}$ for $t_n < t_{n,\kappa} \leq t_{n+1}$ that take into account the convective transport of the water and gas but not the diffusive effects. The algorithm will be detailed below.

The initial conditions S_w and S_g at $t=0$ allow the calculation of $\{p_o^0, \mathbf{v}^0\}$. The following is the fractional step algorithm associated with the differential form of three-phase model that is to be followed until the final simulation time is reached.

Algorithm 3.1: First level

- 1) Given $S_w^m(\mathbf{x})$ and $S_g^m(\mathbf{x})$, $m \geq 0$, determine $\{p_o^m, \mathbf{v}^m\}$ by (2.6)-(2.8), subject to the boundary conditions

$$\begin{aligned} \mathbf{v} \cdot \mathbf{n} &= -q, & \text{for } (x,y) \in \{0\} \times [0,Y], \\ \mathbf{v} \cdot \mathbf{n} &= q, & \text{for } (x,y) \in \{X\} \times [0,Y], \\ \mathbf{v} \cdot \mathbf{n} &= 0, & \text{for } (x,y) \in [0,X] \times (\{0\} \cup \{Y\}), \end{aligned} \quad (3.3)$$

where \mathbf{n} is the unit outer normal vector to $\partial\Omega$. (More general domains and initial and boundary conditions could be treated by our numerical method, but the computational examples are based on the data given above.)

- 2) For $t^m < t \leq t^{m+1}$, solve the convection-diffusion system (2.2)-(2.5) with the initial conditions $S_w(\mathbf{x}, t^m) = S_w^m(\mathbf{x})$ and $S_g(\mathbf{x}, t^m) = S_g^m(\mathbf{x})$; $S_w^m(\mathbf{x})$ and $S_g^m(\mathbf{x})$ are evaluated as the final values of the calculation in $[t^{m-1}, t^m]$ for $m > 0$ or the initial saturations for $m=0$.
-

Algorithm 3.2: Second level

- 1) Let $t_{n_1} = t^m$ and assume that $\{p_o, \mathbf{v}, S_w, S_g\}$ are known for $t \leq t_{n_1}$.
 - 2) For $n = n_1, \dots, n_2 = n_1 + (i_1 - 1)$:
- a) For $\kappa = 0, \dots, (i_2 - 1)$ and $t \in [t_{n,\kappa}, t_{n,\kappa+1}]$, solve the convection system given by (for notational convenience, $s_i^{n,\kappa}$ is replaced by s_i^κ below):

$$\frac{\partial}{\partial t}(\phi(\mathbf{x})s_i^\kappa) + \nabla \cdot [\mathbf{E}(t_{n,\kappa}, \mathbf{v})f_i(s_w^\kappa, s_g^\kappa)] = 0, \quad i=w, g, \quad (3.4)$$

with initial and boundary conditions given by

$$s_i^\kappa(\mathbf{x}, t_{n,\kappa}) = \begin{cases} S_i(\mathbf{x}, t_n), & \kappa=0, \\ s_i^{\kappa-1}(\mathbf{x}, t_{n,\kappa}), & \kappa=1, \dots, i_2-1, \end{cases} \quad i=w, g, \quad (3.5)$$

and

$$[\mathbf{E}(t_{n,\kappa}, \mathbf{v})f_i(s_w^\kappa, s_g^\kappa)] \cdot \mathbf{n} = -qf_i(S_w^L, S_g^L), \quad i=w, g, \quad (x, y) \in \{0\} \times [0, Y], \quad (3.6)$$

where S_w^L , S_g^L are the water and gas saturations of the injected mixture. We remark that $\mathbf{E}(t_{n,\kappa}, \mathbf{v})$ indicates a linear extrapolation operator; it extrapolates to time $t_{n,\kappa}$ the velocity fields \mathbf{v}^{m-1} and \mathbf{v}^m .

- b) Set $\bar{S}_i(\mathbf{x}, t_n) = s_i^{i_2-1}(\mathbf{x}, t_{n,i_2})$, $i=w,g$.
c) Compute the diffusive effects on $[t_n, t_{n+1}]$ by solving the system

$$\frac{\partial}{\partial t}(\phi(\mathbf{x}) S_i) - \nabla \cdot \mathbf{w}_i = 0, \quad i=w,g, \quad (3.7)$$

with boundary conditions

$$\mathbf{w}_i \cdot \mathbf{n} = 0, \quad i=w,g, \quad \mathbf{x} \in \partial\Omega, \quad (3.8)$$

and initial conditions

$$S_i(\mathbf{x}, t_n) = \bar{S}_i(\mathbf{x}, t_n), \quad i=w,g. \quad (3.9)$$

- 3) Set $S_i^{m+1}(\mathbf{x}) = S_i(\mathbf{x}, t_{n_2+1})$, $i=w,g$.
-

Remark 3.1. In Step 2)c) of Algorithm 3.2, the division of the interval $[t_n, t_{n+1}]$ into microsteps of length Δt_c is artificial in the differential case described above, but the division is desirable and often necessary after the full discretization of the convection equations is introduced.

3.1 Numerical procedures

We refer the reader to [29, 34] for a detailed description of the discretization of the governing equations (2.6)-(3.9). Below, we provide the key ideas.

The oil pressure and the Darcy velocity defined by (2.6)-(2.8) are approximated by locally conservative mixed finite elements (see [28, 29]). The linear system of algebraic equations that arises from the discretization of (2.6)-(2.8) is solved by a preconditioned conjugate gradient procedure (PCG) [28, 29].

Locally conservative mixed finite elements are used to discretize the spatial operators in the diffusion system (3.7)-(3.9). The time discretization of the latter is performed by means of the implicit backward Euler method (see for details [29]).

To solve the nonlinear hyperbolic conservation laws (3.4)-(3.5) we use a nonoscillatory, second order, conservative central difference scheme [31] (see also [29, 32]).

4 Numerical simulations

The goal of the numerical experiments reported in this section is to verify the efficiency and accuracy of the proposed operator splitting scheme. We work with the system of Eqs. (2.2)-(2.8) in dimensionless form.

We adopt the model by Corey-Pope [20, 22] for phase relative permeabilities:

$$k_w = S_w^2, \quad k_o = S_o^2 \quad \text{and} \quad k_g = S_g^2. \quad (4.1)$$

We also adopt the Leverett model [35] for capillary pressures given by

$$p_{wo} = 5\epsilon(2 - S_w)(1 - S_w) \quad \text{and} \quad p_{go} = \epsilon(2 - S_g)(1 - S_g), \quad (4.2)$$

where the dimensionless coefficient ϵ controls the relative importance of capillary/diffusive and convective forces. In our numerical experiments we take $\epsilon = 10^{-3}$.

4.1 One-dimensional experiments

In order to verify the efficiency, and mainly, the accuracy of the proposed operator splitting scheme in our one-dimensional experiments, lets consider the following set of data. The viscosities of the fluids are $\mu_o = 1.0$, $\mu_w = 0.5$, and $\mu_g = 0.3$ and we consider the following Riemann initial data with (constant) left and right states given by

$$S_w^L = 0.721, \quad S_w^R = 0.05 \quad \text{and} \quad S_g^L = 0.279, \quad S_g^R = 0.15. \quad (4.3)$$

We remark that for the choice of parameters and initial data described above, a non-classical transitional shock wave appears in the one-dimensional solution of (2.2)-(2.8); (see [36]).

Figs. 1 and 2 show the one-dimensional solution of (2.2)-(2.8) (with Riemann data (4.3)). They display, from top to bottom, saturation values for the oil, gas and water phases, respectively. The computed saturation profiles in these figures were obtained on grids having 512 cells, and are shown at two different dimensionless times.

The left column of Fig. 1 refers to a reference numerical solution, which is in excellent agreement with the semi-analytic results reported in [36]. In this reference solution, the same time step was used in the calculation of convection and diffusion transports, as well as in the pressure-velocity calculation (i.e., $\Delta t_c = \Delta t_d = \Delta t_p$). In the legends of Figs. 1 and 2 the reference solution is denoted by 1:1:1.

The right frames in Fig. 1 compare the numerical solution obtained with the time-step relations $\Delta t_p = \Delta t_d = 50\Delta t_c$ and the reference solution. The left and the right columns of Fig. 2 refer to numerical solutions obtained with the time-step relations $\Delta t_p = \Delta t_d = 100\Delta t_c$ and $\Delta t_p = \Delta t_d = 200\Delta t_c$, respectively.

It is clear from Figs. 1 and 2 that, for the time-step relations considered, the correct transitional wave has been captured, and the numerical solutions virtually coincide with the reference solution, which indicates that the splitting introduced herein produces very accurate results in this test case.

4.2 Two-dimensional experiments

In the next numerical experiment, the fluids flow in a horizontal two-dimensional reservoir $\Omega = [0, X] \times [0, Y]$, with aspect ratio $X/Y = 1$, discretized in a uniform grid of 512 \times 512 cells. A mixture (73.5 % of water and 26.5 % of gas) is injected at constant rate along the left boundary, $(x, y) \in \{0\} \times [0, Y]$, and “no-flow” conditions are imposed on $(x, y) \in [0, X] \times (\{0\} \cup \{Y\})$. Initially, the resident fluid in the reservoir is a mixture of 5% water, 1% gas, and 94% oil; we notice that the initial conditions correspond to the Riemann initial data with (constant) left and right states given by:

$$S_w^L = 0.735, \quad S_w^R = 0.05 \quad \text{and} \quad S_g^L = 0.265, \quad S_g^R = 0.01. \quad (4.4)$$

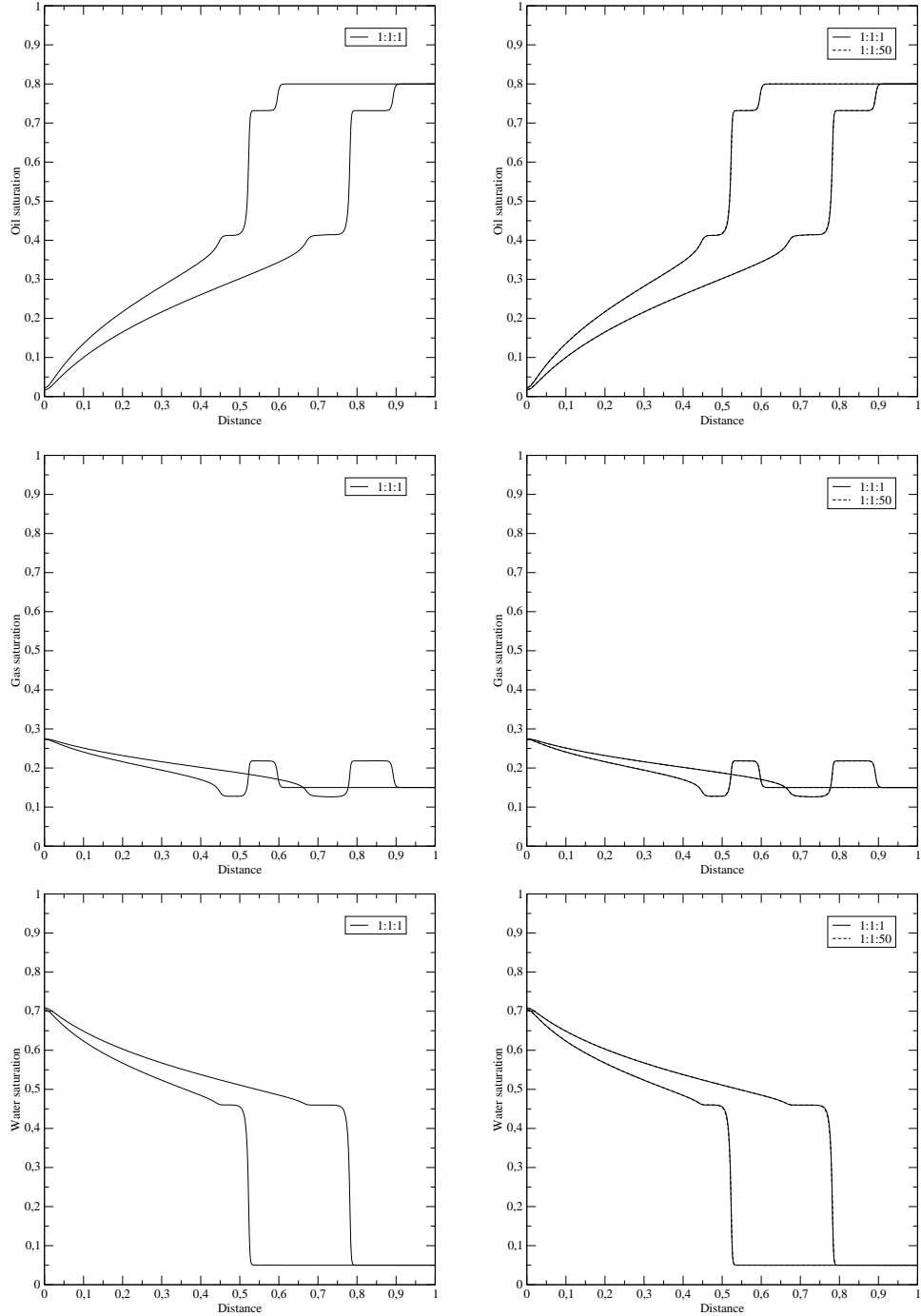


Figure 1: One-dimensional study of the operator splitting scheme. From top to bottom, oil, gas and water saturation profiles are shown as functions of dimensionless distance. On the left the reference run and on the right the time-step relation $\Delta t_p = \Delta t_d = 50\Delta t_c$ is used. A transitional shock wave is simulated.

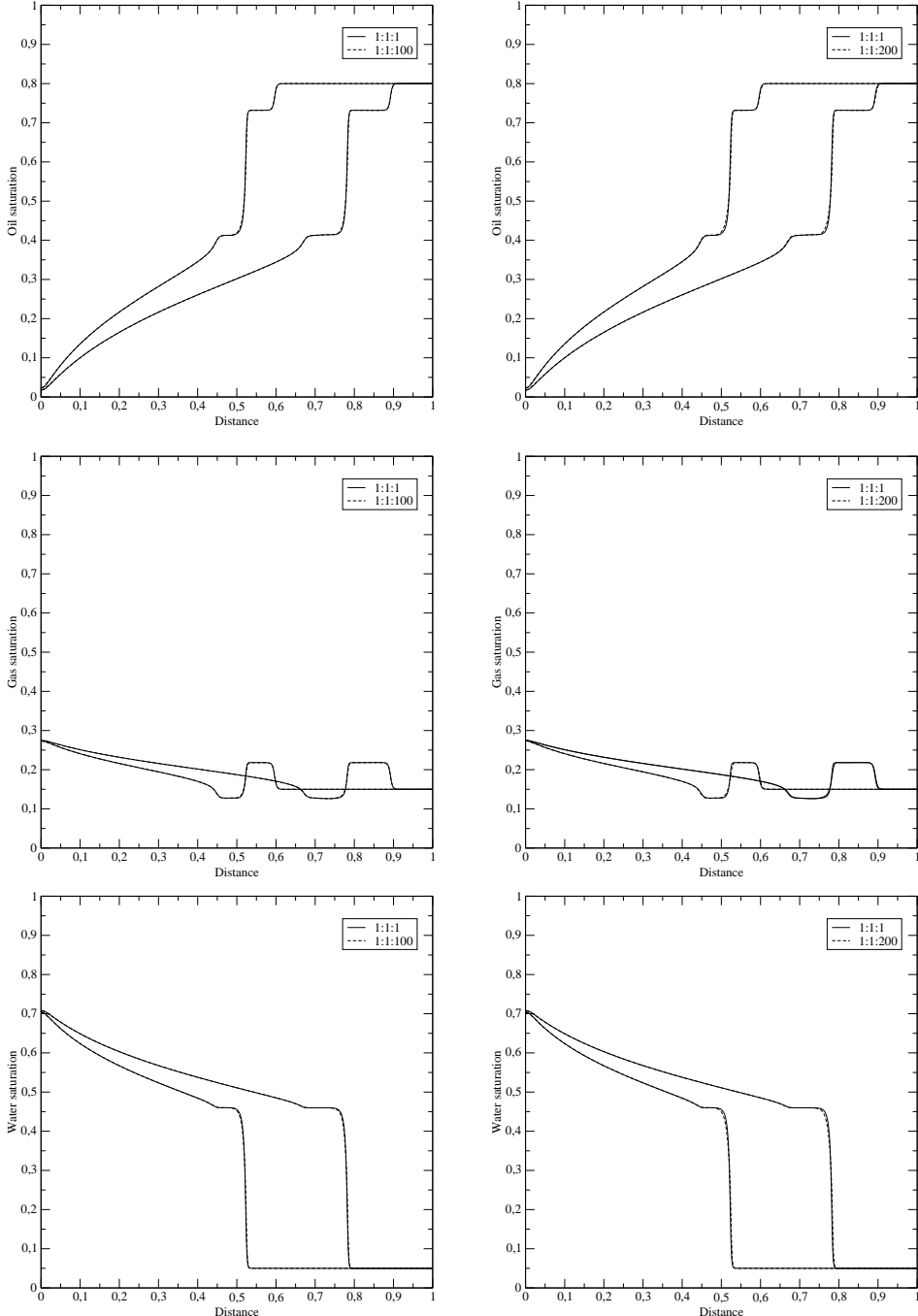


Figure 2: One-dimensional study of the operator splitting scheme. From top to bottom, oil, gas and water saturation profiles are shown as functions of dimensionless distance. On the left the time-step relation $\Delta t_p = \Delta t_d = 100\Delta t_c$ is used and on the right $\Delta t_p = \Delta t_d = 200\Delta t_c$ is considered. Again, a transitional shock wave is accurately simulated.

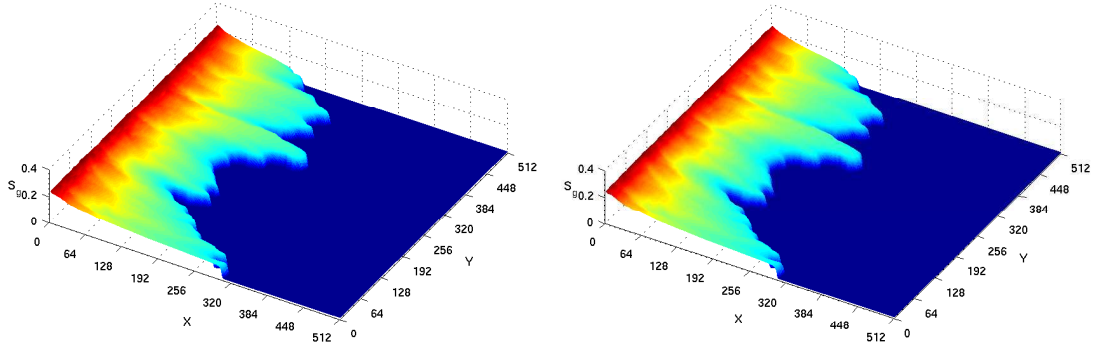


Figure 3: Gas saturation after 500 days is shown for a two-dimensional simulation study using the operator splitting scheme. We consider the following time-step relations: $\Delta t_p = \Delta t_d = \Delta t_c$ (left) and $\Delta t_p = \Delta t_d = 72\Delta t_c$ (right), where Δt_c is determined by a CFL constraint.

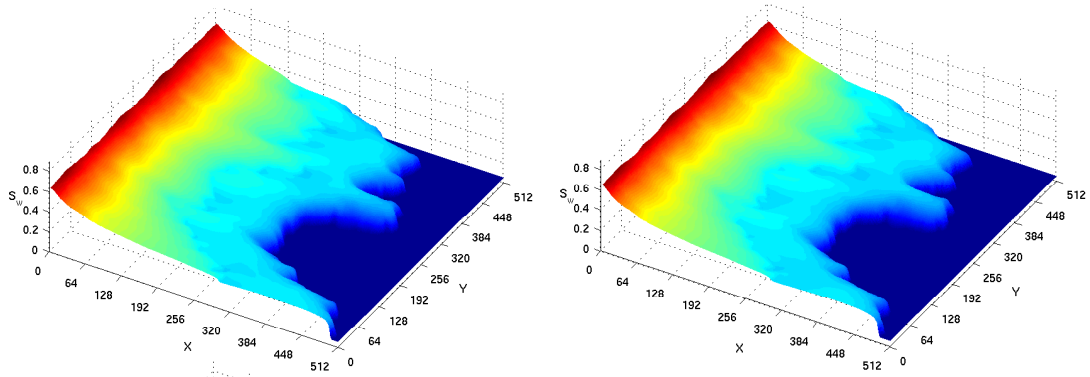


Figure 4: Water saturation surface plots corresponding to the simulation reported in Fig. 3.

In the two-dimensional reservoir flooding problem, we consider more realistic values for the viscosities of the fluids, namely, $\mu_o = 10.0$, $\mu_w = 1.0$ e $\mu_g = 0.5$.

As a model for multiscale rock heterogeneity, we consider scalar, log-normal permeability fields, so that $\xi(\mathbf{x}) = \log K(\mathbf{x})$ is Gaussian and its distribution is determined by its mean and covariance function. We consider a distribution which is stationary, isotropic and fractal (self-similar). Thus, the mean is an absolute constant and the covariance is given by the power law:

$$\text{Cov}(\mathbf{x}, \mathbf{y}) = |\mathbf{x} - \mathbf{y}|^{-\beta}, \quad 0 < \beta < \infty. \quad (4.5)$$

The fractal statistics (4.5) is singular at short distances; however its realization on a finite lattice provides a short distance regularization due to the lattice cutoff. The scaling exponent β controls the nature of multiscale heterogeneity. As it increases, the heterogeneities concentrated in the larger length scales are emphasized and the field becomes locally more regular. A long length scale ($\beta = 0.5$) permeability field with the Gaussian distribution (4.5) was used in the simulations reported in Figs. 3-5.

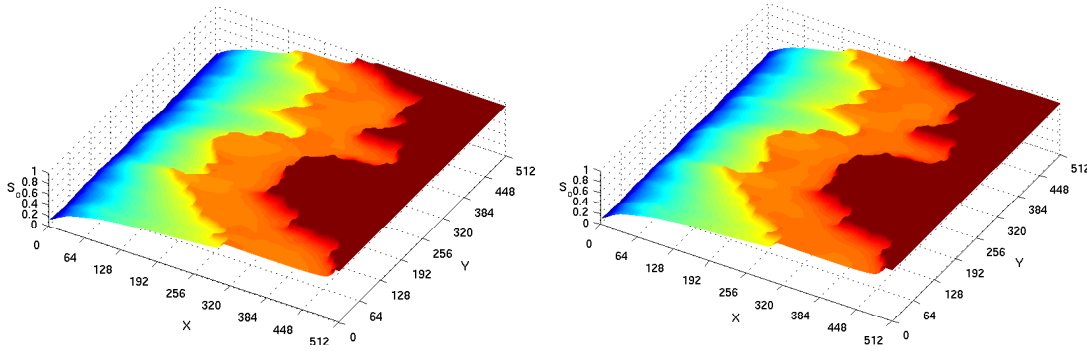


Figure 5: Oil saturation surface plots corresponding to the simulation reported in Fig. 3.

We use the same multiscale rock heterogeneity to construct a variable porosity field $\phi(\mathbf{x})$:

$$\phi(\mathbf{x}) = \bar{\phi} + \theta \xi(\mathbf{x}), \quad \theta > 0, \quad (4.6)$$

where $\bar{\phi} = 0.2$ and the normalizing factor θ is chosen so that $0.05 \leq \phi(\mathbf{x}) \leq 0.35$.

The spatially variable permeability and porosity fields are defined on a uniform geological grid with 512×512 cells and have coefficients of variation ((standard deviation)/mean) $CV_k = 1.0$, and $CV_\phi = 0.25$, respectively. The coefficient of variation serves as a dimensionless measure of the strength of the heterogeneity (permeability and porosity fields).

In Figs. 3-5, gas, water and oil saturation surface plots are shown as functions of position, respectively. For the simulations reported in Figs. 3-5 we take the following time-step relations $\Delta t_p = \Delta t_d = \Delta t_c$ (reference solution on the left) and $\Delta t_p = \Delta t_d = 72\Delta t_c$ (right), where Δt_c is the same for the two tests. Note that even for the largest time-step relation (right pictures in Figs. 3-5) both the small and large scale features of the flow are accurately captured. Obviously, the use of the largest time-step relation translates into a drastically reduced computational effort to produce numerical results within a given accuracy requirement; in the simulations displayed in Figs. 3-5, this reduction entails a time saving of more than 80 %.

5 Conclusions

We have described an accurate and efficient operator splitting technique for the numerical solution of three-phase flow through heterogeneous petroleum reservoirs. The numerical results obtained indicate that the delicate balance between the focusing effects of nonlinear convection, which lead to the formation of shocks, and the smoothing effect of diffusion are captured by our method. Currently the authors are using this simulator to study the scale-up problem for such flows.

References

- [1] Peaceman, D.W., and Rachford, H.H., 1955, The numerical solution of parabolic and elliptic equations. *J. Soc. Indust. Appl. Math.*, 3, 28–41.
- [2] Douglas, J., 1955, On the numerical integration of $\frac{\partial^2 u}{\partial x^2} + \frac{\partial^2 u}{\partial y^2} = \frac{\partial u}{\partial t}$ by implicit methods. *J. Soc. Indust. Appl. Math.*, 3, 42–65.
- [3] Douglas, J., and Peaceman, D.W., 1955, Numerical solution of two-dimensional heat flow problems. *American Institute of Chemical Engineering Journal*, 1, 505–512.
- [4] Douglas, J., and Rachford, H.H., 1960, On the numerical solution of heat conduction problems in two and three space variables. *Transaction of the American Mathematical Society*, 82, 421–439.
- [5] Douglas, J., Peaceman, D.W., and Rachford, H.H., 1959, A method for calculating multi-dimensional immiscible displacement. *Trans. of AIME*, 216, 297–308.
- [6] D'yakonov, E.G., 1961, On an iterative method for the solution of a system of finite-difference equations. *DAN SSSR*, 143, 522–525.
- [7] Yanenko, N.N., 1968, *Méthode à Pas Fractionnaires*, Librairie Armand Colin, Paris.
- [8] Gerritsen, M.G., and Durlofsky, L.J., 2006, Modeling fluid flow in oil reservoirs. *Annual Review of Fluid Mechanics*, 37 (1), 211–238.
- [9] Sarathi, P., 1999, In-situ combustion handbook principles and practices. DOE/PC/91008-0374 Technical report, OSTI ID: 3174. National Petroleum Technology Office, U.S. D.O.E.
- [10] Allen, M.B., 1985, Numerical modelling of multiphase flow in porous media. *Adv. Water Resour.*, 8(4), 162–187.
- [11] Christensen, J.R., Stenby, E.H., and Skauge, A., 1998, Review of WAG field experience. *SPE*, 39883, 357–370.
- [12] Guzmán, R.E., Domenico, G., Fayers, F.J., Aziz, K., and Godi, A., 1994, Three-phase flow in field scale simulations of gas and WAG injections. *SPE European Petroleum Conference*, London, UK., SPE 28897.
- [13] Larsen, J.A., and Skauge, A., 1999, Simulation of the immiscible WAG process using cycle-dependent three-phase relative permeabilities. *Proceedings of the SPE ATCE*, Houston, TX, October 3–6, SPE 56745, 153–166.
- [14] Pope, G.A., 1980, The application of fractional flow theory to enhanced oil recovery. *Soc. Pet. Eng. J. Petrol. Trans. AIME*, 269., 20(3), 191–205.
- [15] Pruess, K., 2003, Numerical simulation of leakage from a geological disposal reservoir for CO_2 , with transitions between super- and sub-critical conditions. In *TOUGH Symposium 2003*, Lawrence Berkeley National Laboratory, Berkeley, California, May 12-14, 1–8.
- [16] Lekhov, A.V. and Shvarov, Y.V., 2002, On the rate of radionuclide migration in groundwater. *Water Resources*, 29(3), 244–251.
- [17] Miller, C.T., Christakos, G., Imhoff, P.T., McBride, J.F., Pedit, J.A., and Trangenstein, J.A., 1998, Multiphase flow and transport modeling in heterogeneous porous media: challenges and approaches. *Adv. Water Resour.*, 21(2), 77–120.
- [18] Peaceman, D. W., 1977, *Fundamentals of Numerical Reservoir Simulation*. Elsevier, Amsterdam.
- [19] Chen, Z. and Ewing, R. E., 1997, Comparison of various formulation of three-phase flow in porous media. *J. Comput. Phys.*, 132, 362–373.
- [20] Corey, A., Rathjens, C., Henderson, J., and Wyllie, M., 1956, Three-phase relative permeability. *Trans. AIME*, 207, 349–351.
- [21] Stone, H. L., 1970, Probability model for estimating three-phase relative permeability. *Petrol.*

- Trans. AIME, 249. JPT, 23(2), 214–218.
- [22] Dria, D.E., Pope, G.A, and Sepehrnoori, K., 1993, Three-phase gas/oil/brine relative permeabilities measured under CO_2 flooding conditions. SPE 20184, 143–150.
 - [23] Juanes, R., and Patzek, T. W., 2004, Three-Phase Displacement Theory: An Improved Description of Relative Permeabilities. SPE Journal, 9(3), 302–313.
 - [24] Isaacson, E., Marchesin, D., and Plohr, B., 1990, Transitional waves for conservation laws. SIAM J. Math. Anal., 21, 837–866.
 - [25] Berre, I., Dahle, H. K., Karlson, K. H., and Nordhaug, H. F., 2002, A streamline front tracking method for two- and three-phase flow including capillary forces. Contemporary Mathematics: Fluid flow and transport in porous media: mathematical and numerical treatment, 295, 49–61.
 - [26] Chen, Z., and Ewing, R. E., 1997, Fully-discrete finite element analysis of multiphase flow in ground-water hydrology. SIAM J. Numer. Anal., 34, 2228–2253.
 - [27] Li, B., Chen, Z., and Huan, G., 2003, The sequential method for the black-oil reservoir simulation on unstructured grids. J. Comput. Phys., 192 (1), 36–72.
 - [28] Douglas, J., Furtado, F., and Pereira, F., 1997, On the numerical simulation of waterflooding of heterogeneous petroleum reservoirs. Comput. Geosci., 1(2), 155–190.
 - [29] Abreu, E., Douglas, J., Furtado, F., Marchesin, D., and Pereira, F., 2006, Three-phase Immiscible displacement in heterogeneous petroleum reservoirs. Mathematics and Computers in Simulation, 73(1-4), 2-20.
 - [30] Abreu, E., Furtado, F., Marchesin, D., and Pereira, F., 2004, Transitional waves in three-phase flows in heterogeneous formations. In: C. T. Miller, M. W. Farthing, W. G. Gray and G. F. Pinder (Eds) Computational Methods for Water Resources, Series: Developments in Water Science, I, 609–620.
 - [31] Nessyahu, N., and Tadmor, E., 1990, Non-oscillatory central differencing for hyperbolic conservation laws. J. Comput. Phys., 87(2) 408–463.
 - [32] Abreu, E. and Furtado, F. and Pereira, F., On the numerical simulation of three-phase flows in heterogeneous porous media. In Lecture Notes in Computer Science, Springer-Verlag, 4395 (2007) 504–517.
 - [33] Abreu, E., Furtado, F., and Pereira, F., 2004, On the numerical simulation of three-phase reservoir transport problems. Transport Theory and Statistical Physics, 33(5-7), 503–526.
 - [34] Abreu, E., Douglas, J., Furtado, F., and Pereira, F., Three-phase immiscible displacement in heterogeneous porous media with gravitational effects. In preparation.
 - [35] Leverett, M.C., and Lewis, W.B., 1941, Steady flow of gas-oil-water mixtures through unconsolidated sands, Trans. of AIME, 142, 107–117.
 - [36] Marchesin, D. and Plohr, B. J., 2001, Wave structure in WAG recovery, Society of Petroleum Engineers Journal 56480, 6(2), 209-219.